Excited States of Nitro-Polypyridine Metal Complexes and Their Ultrafast Decay. Time-Resolved IR Absorption, Spectroelectrochemistry, and TD-DFT Calculations of *fac*-[Re(Cl)(CO)$_3$(5-Nitro-1,10-phenanthroline)]

Anders Gabrielsson,[†,#] Pavel Matousek,[‡] Michael Towrie,[‡] František Hartl,[§] Stanislav Záliš,[||] and Antonín Vlček, Jr.*[,†,||]

Department of Chemistry and Centre for Materials Research, Queen Mary, University of London, Mile End Road, London E1 4NS, United Kingdom, Central Laser Facility, CCLRC Rutherford Appleton Laboratory, Chilton, Didcot, Oxfordshire OX11 0QX, United Kingdom, Molecular Photonic Materials, van't Hoff Institute for Molecular Sciences, University of Amsterdam, Nieuwe Achtergracht 166, NL-1018 WV Amsterdam, The Netherlands, and J. Heyrovský Institute of Physical Chemistry, Academy of Sciences of the Czech Republic, Dolejškova 3, CZ-182 23 Prague, Czech Republic

Received: April 2, 2005; In Final Form: May 13, 2005

The lowest absorption band of *fac*-[Re(Cl)(CO)$_3$(5-NO$_2$-phen)] encompasses two close-lying MLCT transitions. The lower one is directed to LUMO, which is heavily localized on the NO$_2$ group. The UV−vis absorption spectrum is well accounted for by TD-DFT (G03/PBEPBE1/CPCM), provided that the solvent, MeCN, is included in the calculations. Near-UV excitation of *fac*-[Re(Cl)(CO)$_3$(5-NO$_2$-phen)] populates a triplet metal to ligand charge-transfer excited state, ^{3}MLCT, that was characterized by picosecond time-resolved IR spectroscopy. Large positive shifts of the ν(CO) bands upon excitation (+70 cm^{-1} for the A′(1) band) signify a very large charge separation between the Re(Cl)(CO)$_3$ unit and the 5-NO$_2$-phen ligand. Details of the excited-state character are revealed by TD-DFT calculated changes of electron density distribution. Experimental excited-state ν(CO) wavenumbers agree well with those calculated by DFT. The ^{3}MLCT state decays with a ca. 10 ps lifetime (in MeCN) into another transient species, that was identified by TRIR and TD-DFT calculations as an intraligand $^3n\pi^*$ excited state, whereby the electron density is excited from the NO$_2$ oxygen lone pairs to the π^* system of 5-NO$_2$-phen. This state is short-lived, decaying to the ground state with a ∼30 ps lifetime. The presence of an $n\pi^*$ state seems to be the main factor responsible for the lack of emission and the very short lifetimes of ^{3}MLCT states seen in all d^6-metal complexes of nitro-polypyridyl ligands. Localization of the excited electron density in the lowest ^{3}MLCT states parallels localization of the extra electron in the reduced state that is characterized by a very small negative shift of the ν(CO) IR bands (−6 cm^{-1} for A′(1)) but a large downward shift of the ν_s(NO$_2$) IR band. The Re−Cl bond is unusually stable toward reduction, whereas the Cl ligand is readily substituted upon oxidation.

Introduction

Introduction of a NO$_2$ group to a polypyridine ligand in complexes of d^6 metals profoundly changes their photophysical and photochemical properties. Re^I and Ru^{II} complexes of 2,2′-bipyridine (bpy) or 1,10-phenanthroline (phen) and their derivatives generally have long-lived, emissive metal to ligand charge-transfer (MLCT) excited states.[1,2] Nitro-polypyridines are a striking exception. Thus, for example, the complexes [Ru(4-NO$_2$-bpy)$_3$]$^{2+}$, *fac*-[Re(Cl)(CO)$_3$(4,4′-(NO$_2$)$_2$-bpy)], *fac*-[Re(Etpy)(CO)$_3$(4,4′-(NO$_2$)$_2$-bpy)]$^+$ (Etpy = 4-ethylpyridine), *fac*-[Re(Cl)(CO)$_3$(5-NO$_2$-phen)], and [M(CO)$_4$(5-NO$_2$-phen)] (M = Cr, Mo, W) show no emission at room temperature, unlike their bpy or phen counterparts.[3−7] This is usually interpreted as evidence for a very fast nonradiative decay of the ^{3}MLCT excited state and, hence, very short excited-state lifetime. Indeed, the ^{3}MLCT lifetimes[8] of *fac*-[Re(Cl)(CO)$_3$(5-NO$_2$-phen)] (7.6±1.8 ps) and *fac*-[Re(Etpy)(CO)$_3$(5-NO$_2$-phen)]$^+$ (170 ± 20 ps) are approximately 10^4 and 3.8×10^4 times shorter, respectively, than those of the corresponding phen complexes. These effects are usually attributed to localization of the excited electron density at the nitro group, although it is not obvious why this should increase the nonradiative decay rate so much.

The presence of a nitro group also affects photochemical reactivity. The quantum yield of photochemical CO dissociation from [Cr(CO)$_4$(5-NO$_2$-phen)] is 54 times smaller than from [Cr(CO)$_4$(phen)].[7] Other substituents (Cl, Me, Ph) have, by comparison, a negligible effect.[7] On the other hand, nitration of the phen ligand has only a very small effect (1.2-fold decrease)[7] on the quantum yield of the associative[9−12] CO photosubstitution from [W(CO)$_4$(phen)].

Very little information is available on the nature of excited states of nitro-polypyridine complexes of d^6 metals. Picosecond time-resolved visible absorption spectra of *fac*-[Re(L)(CO)$_3$(5-NO$_2$-phen)]$^+$ (L = Etpy, imidazole) show[8] broad bands that resemble spectra of reduced nitro-aromatic radical anions[13] while ν(CO) bands observed in picosecond time-resolved IR (TRIR) spectra[8] are strongly shifted to higher wavenumbers because of formal oxidation of the Re(CO)$_3$ unit. All these features are

* Corresponding author e-mail: a.vlcek@qmul.ac.uk.
† University of London.
‡ CCLRC Rutherford Appleton Laboratory.
§ University of Amsterdam.
|| Academy of Sciences of the Czech Republic.
Current address: Institut für Anorganische Chemie der Universität Stuttgart, Pfaffenwaldring 55, D-70569, Stuttgart, Germany.

10.1021/jp051677h CCC: $30.25
Published on Web 06/28/2005

characteristic[14−22] of a ^{3}MLCT state, which can be qualitatively described as *fac*-[Re^{II}(L)(CO)$_3$(5-NO_2-phen$^{\bullet-}$)]$^+$. The exceptionally large magnitude of the ν(CO) shift upon excitation indicates that the charge separation in the ^{3}MLCT state is much larger than in other *fac*-[Re(L)(CO)$_3$(α-diimine)]$^+$ complexes.[8] For *fac*-[Re(imidazole)(CO)$_3$(5-NO_2-phen)]$^+$, the ^{3}MLCT excited state undergoes two parallel processes: nonradiative decay to the ground state and an imidazole→Re^{II} electron transfer, that leads to a ligand-to-ligand charge-transfer excited state (^{3}LLCT), formulated as *fac*-[Re^{I}(imidazole$^{\bullet+}$)(CO)$_3$(5-NO_2-phen$^{\bullet-}$)]$^+$.[8]

As possible sensitizers, nitro-polypyridine complexes are attractive as very strong excited-state oxidants, although the very short lifetimes make them unsuitable for use in bimolecular processes. Assessment and development of nitro-polypyridine complexes as intramolecular photooxidants require better understanding of the nature, dynamics, and relaxation of their low-lying excited states. Herein, we present results of an IR time-resolved spectroscopic and spectroelectrochemical study of *fac*-[Re(Cl)(CO)$_3$(5-NO_2-phen)], combined with a TD-DFT characterization of low-lying excited and reduced states. It is shown that the ^{3}MLCT excited-state lifetimes are diminished by an intervention of a lower-lying intraligand excited state of an $n\pi^*$ character, that is itself very short-lived.

Experimental Section

Materials. *fac*-[Re(Cl)(CO)$_3$(5-NO_2-phen)] was prepared by standard procedures[6,23,24] and was characterized by comparing ν(CO) and ^{1}H NMR spectra with the literature data. All spectroscopic and spectroelectrochemical experiments were performed in solvents of spectroscopic quality (Aldrich). The supporting electrolyte, tetrabutylammonium hexafluorophosphate (Bu_4NPF_6; Aldrich), was recrystallized twice from absolute ethanol and dried overnight at 80 °C under vacuum.

Picosecond Time-Resolved IR Spectroscopy. Time-resolved IR measurements used the equipment and procedures described in detail previously.[25−29] In short, the sample solution was excited (pumped) with ∼3 μJ pulse energy at 400 nm and magic-angle polarization, using frequency-doubled pulses from a Ti:sapphire laser of ∼150 fs duration (fwhm). The diameter of the irradiated area was ca. 200 μm. TRIR spectra were probed with IR (∼150 fs) pulses obtained by difference-frequency generation. The IR probe pulses cover spectral range ∼200 cm^{-1} wide. The sample solutions were flowed through a 0.5-mm CaF_2 IR cell, which was rastered in two dimensions. Pump and probe beams were less than 200-μm in diameter. The spectral bands observed in TRIR spectra were fitted by Lorentzian functions to determine accurately their center positions and shapes. All spectral and kinetic fitting procedures were performed using Microcal Origin 7 software. The spectra are shown from 2 ps onward, when the early coherence effects have subsided.

Electrochemistry and IR Spectroelectrochemistry. The cyclic voltammograms were recorded on an EG&G PAR Model 270/250 potentiostat. A home-built electrochemical cell was used with a three-electrode system: working electrode (0.5 mm^2 Pt disk), auxiliary electrode (Pt coil), and a pseudoreference electrode (Ag coil). All measurements were performed in acetonitrile (MeCN) at a scan rate of 100 mV s^{-1} with 10^{-1} M Bu_4NPF_6 supporting electrolyte and 1−2 mM concentration of the complex. Redox potentials are reported relative to the ferrocene/ferricenium (Fc/Fc^+) couple. Spectroelectrochemical experiments were performed in CH_3CN, CH_2Cl_2, CD_3CN, or CD_2Cl_2 using an optically transparent thin-layer electrochemical (OTTLE) cell[30] and a Bio-Rad FTS-7 spectrometer (16 scans, resolution of 2 cm^{-1}).

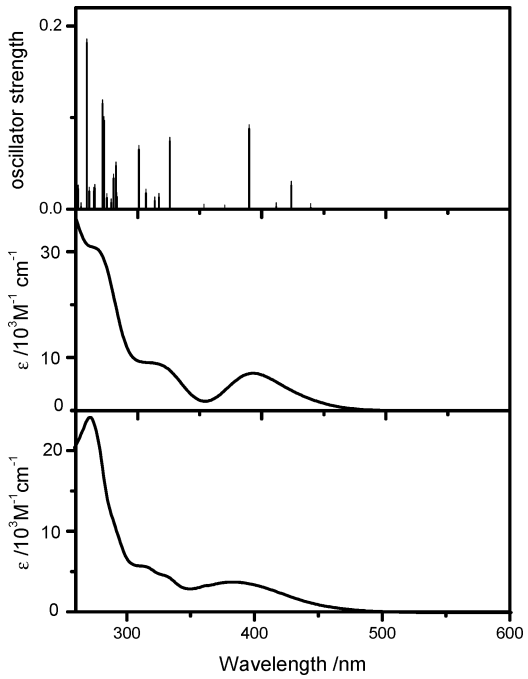

Figure 1. Electronic transitions calculated for *fac*-[Re(Cl)(CO)$_3$(5-NO_2-phen)] in MeCN (top), simulated absorption spectrum (middle), and experimental absorption spectrum measured in MeCN (bottom).

Quantum Chemical Calculations. The electronic structure of *fac*-[Re(Cl)(CO)$_3$(5-NO_2-phen)] was calculated by density functional theory (DFT) methods using the Gaussian 03[31] program package. Low-lying singlet and triplet excited states of the closed-shell complex were calculated by time-dependent DFT (TD-DFT). Calculations of the vibrational frequencies were performed at optimized geometries. Optimization of excited-state geometry was possible only for the lowest triplet state, calculated using the unrestricted Kohn−Sham approach. The polarizable conductor calculation model[32] (CPCM) (G03) was used for modeling of the solvent influence. The difference density plots were prepared using the GaussView software. UV−vis absorption spectra were simulated using the GaussSum[33] software. All calculated transitions are included. Gaussian shapes (0.4 eV fwhm) of the absorption bands were assumed.

For H, C, N, and O atoms, either 6-31G* polarized double ζ basis sets[34] (G03) for geometry optimization and vibrational analysis or cc-pvdz correlation consistent polarized valence double ζ basis sets[35] (TD-DFT) were used, together with quasirelativistic effective core pseudopotentials and corresponding optimized set of basis functions for Re.[36] In all calculations, the hybrid functional using Perdew, Burke, and Ernzerhof[37] exchange and correlation functional with 25% HF exchange (PBE1PBE) was used.

Changes in electron density distribution upon excitation were calculated at the ground-state geometry as electron density differences between the investigated excited state, as described by TD-DFT(G03), and the ground state.

Results

Electronic Transitions. The UV−vis spectrum of [Re(Cl)(CO)$_3$(5-NO_2-phen)] in MeCN (Figure 1, bottom) shows the features typical of [Re(L)(CO)$_3$(α-diimine)] complexes: a broad MLCT band at 383 nm (ϵ = 3700 M^{-1}cm^{-1}) that extends to about 480 nm and a sharp IL band at 271 nm with shoulders at 329 and 312 nm. TD-DFT calculated electronic transitions in MeCN (Figure 1, top, and Table 1) were used to simulate the

TABLE 1: TD-DFT Transition Energies of Low-Lying Singlet Electronic Transitions of *fac*-[Re(Cl)(CO)$_3$(5-NO$_2$-phen)] with Oscillator Strength Larger than 0.001

state	main components (%)	transition energy eV (nm)	osc. str.
b^1A (S_1)	95(HOMO→LUMO); 4(HOMO→LUMO+1)	2.82 (439)	0.002
c^1A (S_2)	99(HOMO-1→LUMO)	2.92 (424)	0.026
d^1A (S_3)	94(HOMO→LUMO+1); 5(HOMO→LUMO)	3.01 (412)	0.002
e^1A (S_4)	97(HOMO-1→LUMO+1)	3.18 (389)	0.088
h^1A (S_5)	40(HOMO-3→LUMO); 25(HOMO-8→LUMO)	3.80 (326)	0.074

absorption spectrum (Figure 1, middle). An excellent agreement with the experimental spectrum was achieved, although the molar absorptivities are somewhat overestimated. Two allowed electronic transitions were calculated to contribute to the lowest absorption band: 2.92 eV (424 nm, oscillator strength = 0.026) and 3.18 eV (389 nm, oscillator strength = 0.088). They correspond to nearly pure one-electron excitations HOMO-1→LUMO and HOMO-1→LUMO+1, respectively. Inspection of the relevant molecular orbitals (Figure 2) shows that both these transitions can be described as MLCT, with a minor contribution from a ligand-to-ligand charge transfer. They differ mostly in the participation of the NO_2 group, which is large for the lowest allowed transition at 2.92 eV but negligible for the higher transition at 3.18 eV.

Picosecond Time-Resolved IR Spectroscopy, TRIR. Shown in Figure 3 are TRIR spectra measured in the ν(CO) region from 2 to 200 ps. Kinetic profiles of individual IR band intensities are plotted in Figure 4. The spectrum recorded at 2 ps after excitation shows negative bands at 1904, 1921, and 2026 cm^{-1} because of the bleached ground-state absorption and transient bands at 1972, ~2010, and 2095 cm^{-1}, which can be directly attributed to an initially formed ^{3}MLCT excited state, because of their similarity with ^{3}MLCT excited-state spectra of analogous Re complexes.[14−22] Characteristically, all three transient ν(CO) bands are strongly shifted to higher wavenumbers from their ground-state positions, and the splitting between the lower two A″ and A′(2) bands increases. Within the next few picoseconds, the ^{3}MLCT spectral features decay with a lifetime of 10.4 ± 0.4 ps, which was determined from the decays of the integrated area of the 2095 cm^{-1} band (10.2 ± 0.4 ps) and of the peak intensity at 1971 cm^{-1} (10.6 ± 0.3 ps). Decay of the ^{3}MLCT bands is accompanied by a growth of two new bands at 2015 and 1886 cm^{-1}, which belong to a secondary transient. These bands reach their maximum intensity at 17−18 ps and then decay with a lifetime of 30.5 ± 2 ps, while the ground state recovers with identical kinetics of 30 ± 1.1 ps, as determined for the relatively isolated 1921 cm^{-1} bleach band (Figure 4).

Detailed inspection of the spectra and kinetic analysis of the early dynamics reveal that the ^{3}MLCT bands narrow and shift slightly to higher wavenumbers, in addition to their intensity decay. This is a typical manifestation of vibrational cooling.[21,38] It is most clearly seen for the highest A′(1) band at 2095 cm^{-1} that initially appears at 2082 cm^{-1} (value extrapolated to t = 0) and shifts to its final position with a biexponential dynamics: 1.4 ± 0.2 ps (8.3 ± 0.9 cm^{-1}) and 7.1 ± 0.7 ps (4.7 ± 0.5 cm^{-1}). The overall dynamic shift is estimated as 13 ± 1 cm^{-1}. Vibrational cooling of the ^{3}MLCT state is also demonstrated by the dependence of the decay kinetics on the probe wavelength: 6.9 ± 0.2 ps at 2086 cm^{-1}, 11.0 ± 0.3 ps at 2091 cm^{-1}, and 14.7 ± 0.5 ps at 2097 cm^{-1}.

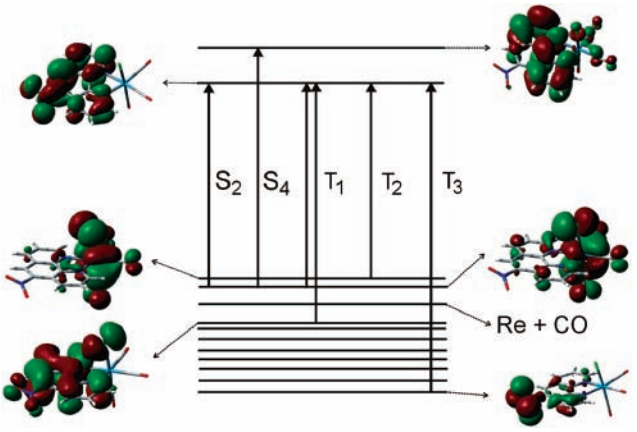

Figure 2. Qualitative scheme of frontier molecular orbitals of *fac*-[Re(Cl)(CO)$_3$(5-NO$_2$-phen)] calculated by DFT in MeCN. The arrows show principal one-electron excitations contributing to the specified low-lying electronic transitions. (Two contributing excitations are shown for T_1, see Table 2).

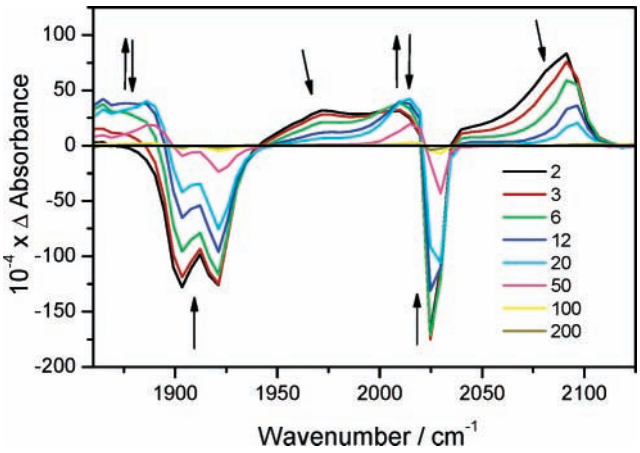

Figure 3. Difference time-resolved IR spectra of *fac*-[Re(Cl)(CO)$_3$(5-NO$_2$-phen)] measured in MeCN after 400 nm excitation. Experimental points are separated by 4−5 cm^{-1}.

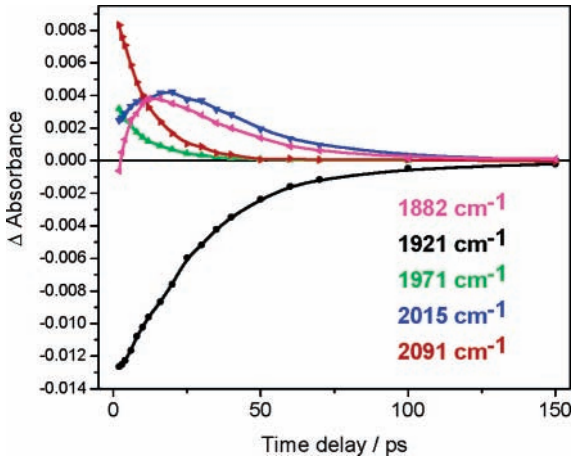

Figure 4. Temporal evolution of IR ν(CO) bands of *fac*-[Re(Cl)(CO)$_3$(5-NO$_2$-phen)] measured in MeCN. The bands due to the initially formed ^{3}MLCT state (2091, 1971 cm^{-1}) decay rapidly while the bands of the secondary transient (2015, 1882 cm^{-1}) increase in intensity. Bleach recovery (1921 cm^{-1}) is concomitant with the decay of the secondary transient (2015, 1882 cm^{-1}).

TABLE 2: TD-DFT Triplet Excitation Energies for [Re(Cl)(CO)$_3$(5-NO$_2$-phen)], Calculated for a MeCN Solution at the Ground-State Geometry

state	main components (%)	transition energy (eV)
a^{3}A (T$_1$)	40(HOMO-3→LUMO); 31(HOMO-1→LUMO)	2.49 (499)
b^{3}A (T$_2$)	96(HOMO→LUMO)	2.77 (448)
c^{3}A (T$_3$)	55(HOMO-10→LUMO); 24(HOMO-10→LUMO+2)	2.83 (437)
d^{3}A (T$_4$)	37(HOMO-1→LUMO); 30(HOMO-1→LUMO+1); 24(HOMO→LUMO+1)	2.87 (431)

The 1886 cm^{-1} band of the secondary transient also shows signs of vibrational dynamics. It is initially formed strongly broadened on its low-wavenumber side. Its growth is accompanied by narrowing and an upward shift, toward its final 1886 cm^{-1} position. The rise and decay time constants both depend on the probe wavelength: 4.5 ± 0.3, 23.7 ± 1.5 ps at 1873 cm^{-1}; 6.8 ± 0.5, 26.2 ± 1.8 ps at 1882 cm^{-1}; and 7.8 ± 0.5, 29.5 ± 1.9 at 1886 cm^{-1}.

TRIR spectra measured in CH_2Cl_2 are very similar to those in MeCN. Weaker signal and broader bands make the kinetic analysis less accurate. Nevertheless, it is obvious that both transients are longer lived than in MeCN. The ^{3}MLCT absorption bands at 1968 and 2082 cm^{-1} decay with a lifetime of 29 ± 5 ps, as measured at 1968 cm^{-1}, into a secondary transient characterized by absorption bands at ca. 1879 (broad) and 2006−2011 cm^{-1}. The latter band grows within the first 30−40 ps and decays completely in 200 ps after excitation. Bleached ground-state bands recover with a 70 ± 7 ps time constant that can be identified with the lifetime of the secondary transient.

TRIR spectra in the region 1475−1605 cm^{-1}, measured in CH_2Cl_2 (Figure 5), show bleaching of the ground-state bands at 1520 and 1543 cm^{-1}, which correspond to vibrations with large $\nu_{as}(NO_2)$ contributions. Two transient bands are seen at ca. 1500 and 1585 cm^{-1}, together with a very broad absorption that overlaps with the bleach bands. The 1500 and 1585 cm^{-1} features shift slightly to higher wavenumbers during the first 20 ps because of vibrational cooling. Although the overall weakness of the TRIR signal prevents a detailed kinetic analysis, it is obvious that the bleach recovery is relatively slow, commensurate with the 70-ps recovery of the ν(CO) features. Only a very broad, poorly resolved transient shifted to lower wavenumbers was observed in the region of the 1318 cm^{-1} ν_s-(NO_2) band.

The low-lying triplet excited states were also investigated computationally, using TD-DFT, see Table 2. It follows that [Re(Cl)(CO)$_3$(5-NO$_2$-phen)] has four triplet states within a narrow energy range 2.49−2.87 eV, calculated at the ground-state geometry. Their characters are revealed by the differences of electron density distribution from the ground state, shown in Figure 6. It follows that a^{3}A (T$_1$) is a Re→5-NO$_2$-phen MLCT state with small 5-NO$_2$-phen $\pi\rightarrow\pi^*$ and Cl→5-NO$_2$-phen LLCT contributions. The b^{3}A (T$_2$) state is a Re→5-NO$_2$-phen MLCT state with a small Cl→5-NO$_2$-phen LLCT component, the excited electron density being heavily localized at the NO_2 group. The c^{3}A (T$_3$) state is localized at the 5-NO$_2$-phen ligand and can be best described as $n\rightarrow\pi^*$, from the oxygen lone electron pairs to the ligand π^* system.

All attempts to optimize triplet excited-state structures by TD-DFT failed, apparently because of the presence of several triplet states of the same symmetry in a very narrow energy range. Hence, TD-DFT calculations alone do not allow us to establish the energy order of triplet excited states at relaxed molecular geometries and actual experimental conditions. Also, it is not possible to simulate excited-state IR spectra using TD-DFT. Calculation using a single-determinant unrestricted Kohn−Sham approach has yielded a ^{3}MLCT lowest excited state whose electron density distribution resembles that of the T$_1$ state, as

TABLE 3: ν(CO) Wavenumbers (cm^{-1}) of the Ground- (GS), ^{3}MLCT Triplet Excited (ES), and One-Electron-Reduced (RS) States of *fac*-[Re(Cl)(CO)$_3$(5-NO$_2$-phen)] Measured and Calculated in a MeCN Solution[a]

GS		ES		RS	
calc.	exp.	calc.	exp.	calc.	exp.
1904	1904	1983	1972	1892	1891
1922	1921	2024	2010	1906	1911
2033	2026	2081	2095	2026	2019

[a] Calculated values are scaled by 0.96 to achieve optimal correspondence for the ground-state values.

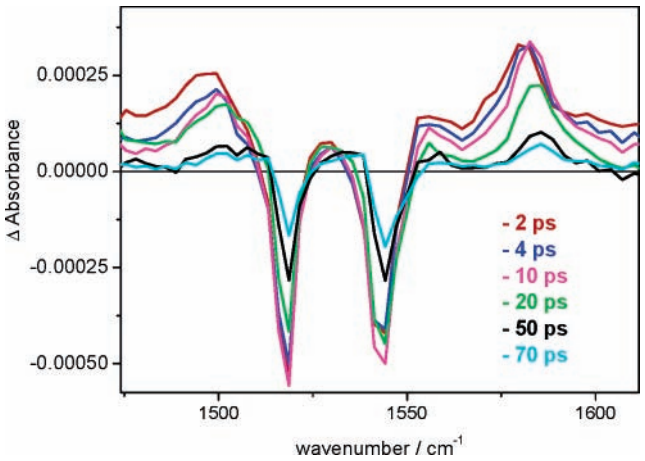

Figure 5. Difference time-resolved IR spectra of *fac*-[Re(Cl)(CO)$_3$-(5-NO$_2$-phen)] in the region of 5-NO$_2$-phen vibrations, measured in CH_2Cl_2 after 400-nm excitation in the region of 5-NO$_2$-phen vibrations. Experimental points are separated by 4−5 cm^{-1}.

Figure 6. Changes of electron density distribution between T$_1$, T$_2$, and T$_3$ excited states and the ground state of *fac*-[Re(Cl)(CO)$_3$(5-NO$_2$-phen)]. Blue and violet colors correspond to a decrease and increase of electron density, respectively. Calculated by TD DFT for MeCN at the ground-state geometry. The Cl atom lies above the Re(5-NO$_2$-phen) plane.

calculated by TD-DFT. The calculated ν(CO) wavenumbers (Table 3) correspond well to the experimental values determined by TRIR for the initially formed transient, confirming its empirical assignment as ^{3}MLCT. No calculated ν(CO) wavenumbers are available for the other low-lying triplet states.

Electrochemistry and IR Spectroelectrochemistry. [Re(Cl)(CO)$_3$(5-NO$_2$-phen)] undergoes fully reversible one-electron reduction in MeCN at $E_{1/2}$ = −1.01 V versus Fc/Fc$^+$, (ΔE_p = 73 mV; identical as for Fc/Fc$^+$ at the same electrode, i_a/i_c = 1 at 100 mV/s). The first reduction potential is ca. 0.7 V more positive than that of [Re(Cl)(CO)$_3$(phen)].[39−41] Such a large shift

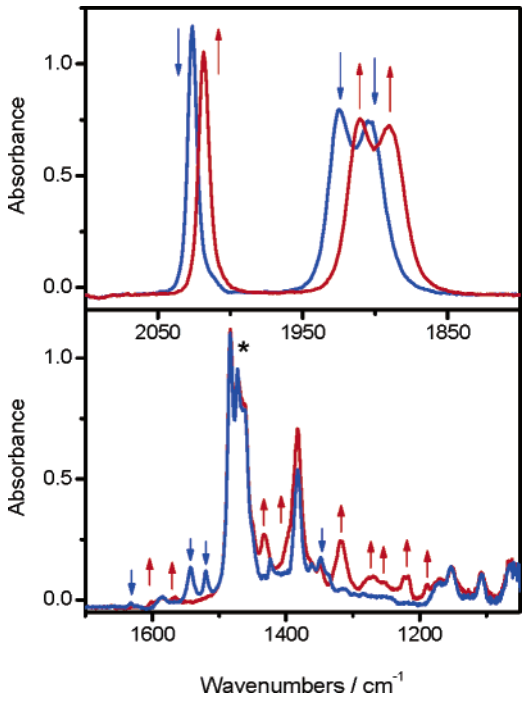

Figure 7. FTIR spectra of *fac*-[Re(Cl)(CO)$_3$(5-NO$_2$-phen)] (blue) and *fac*-[Re(Cl)(CO)$_3$(5-NO$_2$-phen)]$^{\bullet-}$ (red) determined spectroelectrochemically in CD_2Cl_2, in the presence of 0.3 M Bu_4NPF_6 at 293 K. Top: ν(CO) region, see the text. Bottom: region of 5-NO$_2$-phen ligand vibrations. The neutral complex shows bands at 1633, 1543, and 1520 cm^{-1} (ν_{as}(NO$_2$)), ~1338 cm^{-1} (ν_s(NO$_2$)), which disappear upon reduction, being replaced by anion bands at 1603 (w), 1567 (w), 1433 (s), 1389 (s), 1319 (s), 1270 (m), 1257 (w), 1224+1218 (m), 1191 (m), and 1141 (w) cm^{-1}.

upon nitration indicates a heavy localization of the extra electron density on the NO$_2$ group. Second one-electron reduction at $E_{1/2}$ = −1.68 V is electrochemically quasireversible (ΔE_p = 120 mV) and the product is stable at scan rates faster than 100 mV/s.

IR spectra monitored in the course of the first reduction of [Re(Cl)(CO)$_3$(5-NO$_2$-phen)] show (Figure 7) a clean isosbestic conversion of the parent IR ν(CO) pattern (2026, 1925, and 1905 cm^{-1} in CD_2Cl_2) to that of the reduction product characterized by bands at 2019, 1910, and 1890 cm^{-1}. An identical picture is observed in MeCN, where the parent ν(CO) bands at 2026, 1920, and 1904 cm^{-1} are isosbestically replaced upon reduction by those at 2019, 1911, and 1891 cm^{-1}. The observed downward shift of ν(CO) wavenumbers is about 3 times smaller than that seen[42] for an analogous [Re(Cl)(CO)$_3$-(bpy)] complex, indicating that the extra electron density in the reduced [Re(Cl)(CO)$_3$(5-NO$_2$-phen)]$^{\bullet-}$ is predominantly located on the NO$_2$ group, remote from the Re center. This conclusion is fully supported by DFT calculations, which well reproduce the ν(CO) shift upon reduction, see Table 3. The calculated change of electron density distribution upon reduction (Figure 8) clearly documents the localization of the extra electron density in the π^* system of the 5-NO$_2$-phen ligand and, especially, at the NO$_2$ group. This conclusion is further supported by the replacement of the weak ν_s(NO$_2$) band at ~1338 cm^{-1} with an intense band at 1319 cm^{-1} and a medium-intensity band at 1218−1224 cm^{-1} upon reduction. DFT calculation of the reduced complex indicates a large coupling between ν_s(NO$_2$) and phen-ring vibrations. In accord with the experiment, two vibrations with large ν_s(NO$_2$) contributions were calculated at 1300 and 1281 cm^{-1} for [Re(Cl)(CO)$_3$(5-NO$_2$-phen)]$^{\bullet-}$.

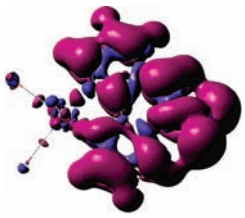

Figure 8. Change of electron density distribution in the course of [Re-(Cl)(CO)$_3$(5-NO$_2$-phen)] reduction. Blue and violet colors correspond to a decrease and increase of electron density, respectively. The Cl atom lies above the plane and the NO$_2$ group points down. Calculated by TD-DFT for MeCN.

The stability of the Re−Cl bond upon the first and second reduction is remarkable and contrasts the behavior seen for other [Re(Cl)(CO)$_3$(α-diimine)] complexes.[39−43] This is the consequence of the localization of the extra electron density on the NO$_2$ group, remote from the Re−Cl moiety.

[Re(Cl)(CO)$_3$(5-NO$_2$-phen)] also undergoes one-electron, chemically irreversible, oxidation $E_{p,a}$ = +1.03 V versus Fc/Fc$^+$ (in MeCN). The shape of the voltammetric wave suggests a diffusion-controlled process followed by a very fast chemical reaction. Second, quasireversible anodic wave $E_{1/2}$ = +1.46 V (ΔE_p = 119 mV) corresponds to oxidation of [Re(MeCN)(CO)$_3$-(5-NO$_2$-phen)]$^+$, formed after the first oxidation step.[41] This is confirmed by IR oxidative spectroelectrochemistry which shows a rapid and clean conversion of [Re(Cl)(CO)$_3$(5-NO$_2$-phen)] to [Re(MeCN)(CO)$_3$(5-NO$_2$-phen)]$^+$, characterized by bands at 2044 (A′(1)) and 1941 (br, A′(2)+A″) cm^{-1} at potentials slightly more positive then +1.03 V. The IR spectrum in the region of 5-NO$_2$-phen vibrations remains unchanged. Such an oxidative labilization of a Re−Cl bond in [Re(Cl)(CO)$_3$(5-NO$_2$-phen)], whereby the Cl$^-$ ligand is oxidized and replaced by MeCN, was already established for [Re(Cl)(CO)$_3$(phen)], and its bpy counterpart.[41] It follows that the HOMO, from which the electron is abstracted, has a large Cl p_π contribution, in accordance with the DFT calculation (Figure 2).

Discussion

The UV−vis absorption spectrum and TD-DFT calculations show that the low-lying allowed singlet transitions of [Re(Cl)-(CO)$_3$(5-NO$_2$-phen)] are MLCT with a small Cl→5-NO$_2$-phen LLCT contribution, similarly to other [Re(Cl)(CO)$_3$(α-diimine)] complexes.[1] Compared with [Re(Cl)(CO)$_3$(phen)], the oxidation and reduction occurs more positively by 0.42 and 0.70 V, respectively, while the maximum of the MLCT absorption band shifts from 364 to 384 nm, that is, by about −0.18 eV.[39,41]

As was discussed in the Introduction, the complexes of nitrated polypyridine ligands differ from their polypyridine counterparts by the lack of emission and very short excited-state lifetimes. Herein, we have clearly identified the initially populated excited state as ^{3}MLCT, see Scheme 1. The upward shift of ν(CO) wavenumbers from the ground-state values is the largest one seen for any [Re(L)(CO)$_3$(α-diimine)] complex, +70 cm^{-1} for the highest A′(1) ν(CO) band. For comparison, shifts of +33 cm^{-1}, +40 cm^{-1}, and +54 cm^{-1} were reported for [Re(Etpy)(CO)$_3$(phen)]$^+$, [Re(Cl)(CO)$_3$(bpy)], and [Re-(Etpy)(CO)$_3$(4,4′-{COOEt}$_2$-2,2′-bpy]$^+$, respectively.[8,15,20] This observation points to a very large charge separation between the Re(Cl)(CO)$_3$ unit and the 5-NO$_2$-phen ligand in the ^{3}MLCT excited state of [Re(Cl)(CO)$_3$(5-NO$_2$-phen)], where the excited electron density is largely localized at the NO$_2$ group, remote from the Re atom. This conclusion is further supported by TD-

SCHEME 1: Excited State Behavior of *fac*-[Re(Cl)(CO)$_3$(5-NO$_2$-phen)][a]

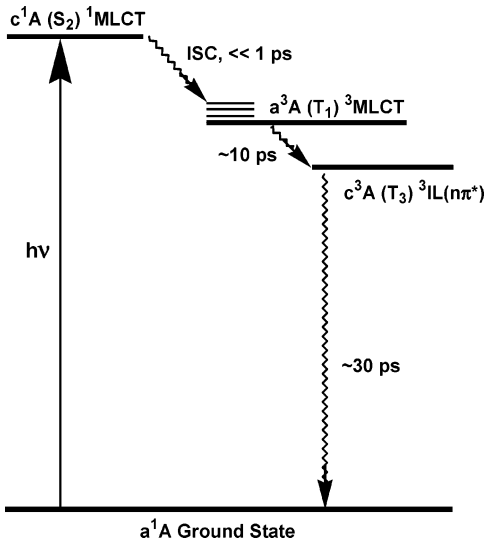

[a] Optical excitation populates the ^{1}MLCT excited state, from which the ^{3}MLCT state is populated by a femtosecond intersystem crossing. The ^{3}MLCT state undergoes a ~10 ps internal conversion to a close-lying intraligand state of an $n\pi^*$ character, which decays to the ground state with a ca. 30 ps lifetime (in MeCN). Excited-state notation corresponds to that used in Tables 1 and 2. The energy order of the relaxed triplet states is assumed to be different from that calculated at the ground-state geometry (see the text).

DFT calculated changes of electron density distribution, Figure 6. However, the large charge separation itself cannot explain the short ^{3}MLCT lifetime, 8−10 ps.

TRIR spectra show that the ^{3}MLCT state of [Re(Cl)(CO)$_3$(5-NO$_2$-phen)] decays to another transient, characterized by ν(CO) bands with wavenumbers shifted slightly downward relative to the ground state: −11 cm^{-1} for the A′(1) band. Such behavior indicates that the secondary transient, populated from the ^{3}MLCT state, could be an LLCT state (Cl→5-NO$_2$-phen), a vibrationally hot ground state, or an intraligand (^{3}IL) state. Assignment of the secondary transient as ^{3}LLCT is effectively excluded by TD-DFT which did not find any such state in the relevant energy range. Moreover, the time-resolved visible absorption spectrum[8] does not show any features attributable to 5-NO$_2$-phen$^{\bullet-}$ that would outlive the ^{3}MLCT state. The second possibility, population of a vibrationally hot ground state, cannot be addressed by DFT calculations. Such a mechanism has not been observed for any other Re carbonyl complex. Hence, it would have to arise from an extremely strong coupling between the ^{3}MLCT state and vibrations of the NO$_2$ group, which seems rather unlikely. In fact, there are more arguments against this mechanism: (i) Vibrational cooling of the ^{3}MLCT state, manifested by the dynamic downward shift of the A′(1) band at early times after excitation, is very similar to that observed[8,21,22,38] for complexes such as [Re(Cl)(CO)$_3$(bpy)], [Re(4-Etpy)(CO)$_3$(bpy)]$^+$, [Re(4-benzoyl-pyridine)(CO)$_3$(bpy)]$^+$, or [Re(4-Etpy)(CO)$_3$(bpy)]$^+$, whose ^{3}MLCT state decays relatively slowly, without any intermediates. (ii) The higher IR band of the secondary transient at 2015 cm^{-1} is not broadened and decays without any shift of its position, opposite to what would be expected for a vibrationally hot species. (iii) The ^{3}MLCT decay and bleach recovery are strongly solvent dependent. Solvent could affect the rate of vibrational cooling (i.e., bleach recovery), but it is not expected to affect much the rate of population of a vibrationally hot ground state. The ~30 ps ^{3}MLCT lifetime seen in CH$_2$Cl$_2$ is rather long for a conversion to a hot ground state. It would require that the vibrational excitation is preserved for much longer, in contrast with the observed <10 ps ^{3}MLCT vibrational cooling.

It is thus proposed that the secondary transient seen in the TRIR spectra is an intraligand state, ^{3}IL, of an $n\pi^*$ origin. This conclusion is strongly supported by TD-DFT calculations (Table 2), which reveal the presence of such a state, c^{3}A, at a relatively low energy. It was calculated as the third triplet (T$_3$) at the ground-state geometry, lying very close, 0.34 eV, above the lowest triplet state. It is conceivable that it becomes the lowest triplet state at the relaxed excited-state geometry. However, this hypothesis could not have been tested computationally since calculations of relaxed triplet states by TD-DFT failed and the single-determinant approach is too crude to determine reliably which state is the lowest. However, the proposed $^3n\pi^*$ intraligand character of the secondary transient is qualitatively supported by the observed downward shift of ν(CO) bands, which is caused by a decrease in π back-bonding to the 5-NO$_2$-phen ligand upon population of the ligand π^* orbital.[44] Further support for the presence of an $n\pi^*$ comes from UV absorption and luminescence spectra of organic nitroaromatic compounds.[45,46]

The presence of an intraligand $^3n\pi$ state, which lies only slightly below ^{3}MLCT, provides a deactivation pathway for the ^{3}MLCT state, see Scheme 1. Conversion to the $^3n\pi^*$ state is much faster than the usual decay to the ground state, decreasing the ^{3}MLCT lifetime by more than 3 orders of magnitude compared with analogous complexes that do not contain a nitro group. Because of its $n\pi^*$ character, the intraligand state undergoes rapid nonradiative conversion to the ground state, Scheme 1. This mechanism can be generalized and used to explain the lack of emission and short excited-state lifetimes typical for nitro-polypyridine complexes of d^6 metals. It is also suggested that ^{3}MLCT lifetimes of nitro-polypyridyl complexes can be prolonged either by increasing the ^{3}IL energy (e.g., by protonation) or by lowering the ^{3}MLCT energy by a judicious choice of the metal (e.g., Os^{II}) or the ancillary ligands.

It is interesting to compare excited-state behavior of [Re(Cl)(CO)$_3$(5-NO$_2$-phen)] with the analogous complexes [Re(Etpy)(CO)$_3$(5-NO$_2$-phen)]$^+$ and [Re(imidazole)(CO)$_3$(5-NO$_2$-phen)]$^+$. Their excitation also populates ^{3}MLCT excited states, which are characterized by very large ν(CO) shifts, indicating large charge separation.[8] The ^{3}MLCT state of [Re(Etpy)(CO)$_3$(5-NO$_2$-phen)]$^+$ decays to the ground state without any observable intermediate with a lifetime of 170 ps[8] that is at least 9000-times faster than the analogous phen complex. The ^{3}MLCT decay most probably proceeds through the same ^{3}IL $n\pi^*$ state as proposed above for [Re(Cl)(CO)$_3$(5-NO$_2$-phen)]. However, the ^{3}IL $n\pi^*$ state of [Re(Etpy)(CO)$_3$(5-NO$_2$-phen)]$^+$ cannot be detected since its lifetime is much shorter than that of the ^{3}MLCT state. For [Re(imidazole)(CO)$_3$(5-NO$_2$-phen)]$^+$ complex, the ^{3}MLCT state decays (43 ps in MeCN) through a transient whose IR spectrum resembles that of the ^{3}IL $n\pi^*$ state discussed herein, although it is rather weak in CH$_3$CN.[8] The TRIR spectrum of the secondary transient in D$_2$O is somewhat different, showing larger downward IR ν(CO) shifts and a weak absorption in the visible because of 5-NO$_2$-phen$^{\bullet-}$.[8] This behavior was attributed[8] to an imidazole→5-NO$_2$-phen ^{3}LLCT state. In view of the results presented above, it appears that both imidazole→5-NO$_2$-phen ^{3}LLCT and ^{3}IL $n\pi^*$ states are involved in the [Re(imidazole)(CO)$_3$(5-NO$_2$-phen)]$^+$ photophysics, their relative contributions being solvent-dependent.

Conclusions

Optical excitation of $[Re(Cl)(CO)_3(5\text{-}NO_2\text{-phen})]$ leads to population of a ^{3}MLCT excited state (Scheme 1), whereby the excited electron density is strongly shifted to the 5-NO_2-phen ligand, in particular, to the NO_2 group. The presence of a lower-lying ^{3}IL $n\pi^*$ excited state is the most probable reason for the unusually short (picosecond) lifetimes of ^{3}MLCT excited states in nitro-polypyridyl complexes of d^6 metals such as Re^I or Ru^{II}. For $[Re(Cl)(CO)_3(5\text{-}NO_2\text{-phen})]$, the ^{3}MLCT state undergoes a ~10 ps conversion to the ^{3}IL $n\pi^*$ state which is short-lived and decays to the ground state with lifetimes of ~30 and ~70 ps in MeCN and CH_2Cl_2, respectively, see Scheme 1. The ^{3}IL $n\pi^*$ state is characterized by a lack of absorption in the visible spectral region, ν(CO) IR bands that are shifted slightly downward from their ground-state positions, and a short (ps) lifetime.

The extra electron density in the reduced complex $[Re(Cl)(CO)_3(5\text{-}NO_2\text{-phen})]^{\bullet-}$ is heavily localized on the NO_2 group, resembling the excited electron density in the lowest ^{3}MLCT state. This localization results in a remarkable stability of the Re−Cl bond upon reduction.

Acknowledgment. Funding and support from the COST Action D14, CCLRC Rutherford Appleton Laboratory and QMUL, and the Ministry of Education of the Czech Republic are gratefully acknowledged.

References and Notes

(1) Stufkens, D. J.; Vlček, A., Jr. *Coord. Chem. Rev.* **1998**, *177*, 127−179.

(2) Juris, A.; Balzani, V.; Barigelletti, F.; Campagna, S.; Belser, P.; von Zelewsky, A. *Coord. Chem. Rev.* **1988**, *84*, 85−277.

(3) Basu, A.; Weiner, M. A.; Strekas, T. C.; Gafney, H. D. *Inorg. Chem.* **1982**, *21*, 1085−1092.

(4) Juris, A.; Campagna, S.; Bidd, I.; Lehn, J.-M.; Ziessel, R. *Inorg. Chem.* **1988**, *27*, 4007−4011.

(5) Hino, J. K.; Della Ciana, L.; Dressick, W. J.; Sullivan, B. P. *Inorg. Chem.* **1992**, *31*, 1072−1080.

(6) Wrighton, M. S.; Morse, D. L. *J. Am. Chem. Soc.* **1974**, *96*, 998−1003.

(7) Manuta, D. M.; Lees, A. J. *Inorg. Chem.* **1986**, *25*, 1354−1359.

(8) Busby, M.; Matousek, P.; Towrie, M.; Di Bilio, A. J.; Gray, H. B.; Vlček, A. J. *Inorg. Chem.* **2004**, *43*, 4994−5002.

(9) Wieland, S.; Reddy, K. B.; van Eldik, R. *Organometallics* **1990**, *9*, 1802−1806.

(10) Fu, W.-F.; van Eldik, R. *Inorg. Chem.* **1998**, *37*, 1044−1050.

(11) Fu, W. F.; van Eldik, R. *Organometallics* **1997**, *16*, 572−578.

(12) van Dijk, H. K.; Servaas, P. C.; Stufkens, D. J.; Oskam, A. *Inorg. Chim. Acta* **1985**, *104*, 179−183.

(13) Shida, T. *Physical Sciences Data 34. Electronic Absorption Spectra of Radical Ions*; Elsevier: Amsterdam-Oxford-New York-Tokyo, 1988.

(14) Glyn, P.; George, M. W.; Hodges, P. M.; Turner, J. J. *J. Chem. Soc., Chem. Commun.* **1989**, 1655−1657.

(15) George, M. W.; Johnson, F. P. A.; Westwell, J. R.; Hodges, P. M.; Turner, J. J. *J. Chem. Soc., Dalton Trans.* **1993**, 2977−2979.

(16) Gamelin, D. R.; George, M. W.; Glyn, P.; Grevels, F.-W.; Johnson, F. P. A.; Klotzbücher, W.; Morrison, S. L.; Russell, G.; Schaffner, K.; Turner, J. J. *Inorg. Chem.* **1994**, *33*, 3246−3250.

(17) Bignozzi, C. A.; Schoonover, J. R.; Dyer, R. B. *Comments Inorg. Chem.* **1996**, *18*, 77−100.

(18) Schoonover, J. R.; Strouse, G. F.; Omberg, K. M.; Dyer, R. B. *Comments Inorg. Chem.* **1996**, *18*, 165−188.

(19) Schoonover, J. R.; Strouse, G. F. *Chem. Rev.* **1998**, *98*, 1335−1355.

(20) Dattelbaum, D. M.; Omberg, K. M.; Schoonover, J. R.; Martin, R. L.; Meyer, T. J. *Inorg. Chem.* **2002**, *41*, 6071−6079.

(21) Liard, D. J.; Busby, M.; Matousek, P.; Towrie, M.; Vlček, A., Jr. *J. Phys. Chem. A* **2004**, *108*, 2363−2369.

(22) Busby, M.; Matousek, P.; Towrie, M.; Clark, I. P.; Motevalli, M.; Hartl, F.; Vlček, A., Jr. *Inorg. Chem.* **2004**, *43*, 4523−4530.

(23) Fredericks, S. M.; Luong, J. C.; Wrighton, M. S. *J. Am. Chem. Soc.* **1979**, *101*, 7415−7417.

(24) Wallace, L.; Rillema, D. P. *Inorg. Chem.* **1993**, *32*, 3836−3843.

(25) Matousek, P.; Towrie, M.; Stanley, A.; Parker, A. W. *Appl. Spectrosc.* **1999**, *53*, 1485−1489.

(26) Matousek, P.; Towrie, M.; Ma, C.; Kwok, W. M.; Phillips, D.; Toner, W. T.; Parker, A. W. *J. Raman Spectrosc.* **2001**, *32*, 983−988.

(27) Towrie, M.; Grills, D. C.; Dyer, J.; Weinstein, J. A.; Matousek, P.; Barton, R.; Bailey, P. D.; Subramaniam, N.; Kwok, W. M.; Ma, C. S.; Phillips, D.; Parker, A. W.; George, M. W. *Appl. Spectrosc.* **2003**, *57*, 367−380.

(28) Vlček, A., Jr.; Farrell, I. R.; Liard, D. J.; Matousek, P.; Towrie, M.; Parker, A. W.; Grills, D. C.; George, M. W. *J. Chem. Soc., Dalton Trans.* **2002**, 701−712.

(29) Liard, D. J.; Busby, M.; Farrell, I. R.; Matousek, P.; Towrie, M.; Vlček, A., Jr. *J. Phys. Chem. A* **2004**, *108*, 556−567.

(30) Krejčík, M.; Daněk, M.; Hartl, F. *J. Electroanal. Chem., Interfacial Electrochem.* **1991**, *317*, 179−187.

(31) Frisch, M. J.; Trucks, G. W.; Schlegel, H. B.; Scuseria, G. E.; Robb, M. A.; Cheeseman, J. R.; J. A. Montgomery, J.; Vreven, T.; Kudin, K. N.; Burant, J. C.; Millam, J. M.; Iyengar, S. S.; Tomasi, J.; Barone, V.; Mennucci, B.; Cossi, M.; Scalmani, G.; Rega, N.; Petersson, G. A.; Nakatsuji, H.; Hada, M.; Ehara, M.; Toyota, K.; Fukuda, R.; Hasegawa, J.; Ishida, M.; Nakajima, T.; Honda, Y.; Kitao, O.; Nakai, H.; Klene, M.; Li, X.; Knox, J. E.; Hratchian, H. P.; Cross, J. B.; Bakken, V.; Adamo, C.; Jaramillo, J.; Gomperts, R.; Stratmann, R. E.; Yazyev, O.; Austin, A. J.; Cammi, R.; Pomelli, C.; Ochterski, J. W.; Ayala, P. Y.; Morokuma, K.; Voth, G. A.; Salvador, P.; Dannenberg, J. J.; Zakrzewski, V. G.; Dapprich, S.; Daniels, A. D.; Strain, M. C.; Farkas, O.; Malick, D. K.; Rabuck, A. D.; Raghavachari, K.; Foresman, J. B.; Ortiz, J. V.; Cui, Q.; Baboul, A. G.; Clifford, S.; Cioslowski, J.; Stefanov, B. B.; Liu, G.; Liashenko, A.; Piskorz, P.; Komaromi, I.; Martin, R. L.; Fox, D. J.; Keith, T.; Al-Laham, M. A.; Peng, C. Y.; Nanayakkara, A.; Challacombe, M.; Gill, P. M. W.; Johnson, B.; Chen, W.; Wong, M. W.; Gonzalez, C.; Pople, J. A. *Gaussian 03*, Revision C.02; Gaussian, Inc., 2004.

(32) Cossi, M.; Rega, N.; Scalmani, G.; Barone, V. *J. Comput. Chem.* **2003**, *24*, 669.

(33) O'Boyle, N. M.; Vos, J. G. *GaussSum 0.8*; Dublin City University, 2004.

(34) Hariharan, P. C.; Pople, J. A. *Theor. Chim. Acta* **1973**, *28*, 213.

(35) Woon, D. E.; Dunning, T. H., Jr. *J. Chem. Phys.* **1993**, *98*, 1358.

(36) Andrae, D.; Häussermann, U.; Dolg, M.; Stoll, H.; Preuss, H. *Theor. Chim. Acta* **1990**, *77*, 123−141.

(37) Perdew, J. P.; Burke, K.; Ernzerhof, M. *Phys. Rev. Lett.* **1996**, *77*, 3865.

(38) Asbury, J. B.; Wang, Y.; Lian, T. *Bull. Chem. Soc. Jpn.* **2002**, *75*, 973−983.

(39) Kalyanasundaram, K. *J. Chem. Soc., Faraday Trans. 2* **1986**, *82*, 2401−2415.

(40) Luong, J. C.; Nadjo, L.; Wrighton, M. S. *J. Am. Chem. Soc.* **1978**, *100*, 5790.

(41) Paolucci, F.; Marcaccio, M.; Paradisi, C.; Roffia, S.; Bignozzi, C. A.; Amatore, C. *J. Phys. Chem. B* **1998**, *102*, 4759−4769.

(42) Johnson, F. P. A.; George, M. W.; Hartl, F.; Turner, J. J. *Organometallics* **1996**, *15*, 3374−3387.

(43) Stor, G. J.; Hartl, F.; van Outersterp, J. W. M.; Stufkens, D. J. *Organometallics* **1995**, *14*, 1115−1131.

(44) Dattelbaum, D. M.; Omberg, K. M.; Hay, P. J.; Gebhart, N. L.; Martin, R. L.; Schoonover, J. R.; Meyer, T. J. *J. Phys. Phem. A* **2004**, *108*, 3527−3536.

(45) Abbott, J. E.; Peng, X.; Kong, W. *J. Chem. Phys.* **2002**, *117*, 8670−8675.

(46) Khalil, O. S.; Bach, H. G.; McGlynn, S. P. *J. Mol. Spectrosc.* **1970**, *35*, 455−460.